

System size dependence of hydration shell occupancy

D. Asthagiri*,† and Dheeraj Singh Tomar*,‡

*Department of Chemical and Biomolecular Engineering, Rice University, Houston, TX

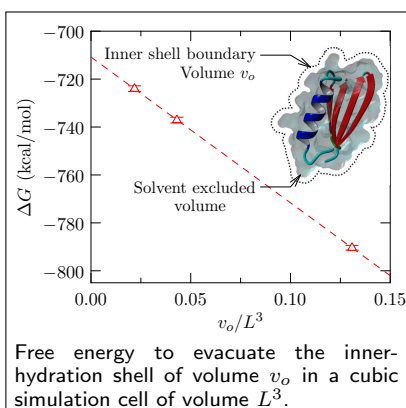
‡Akrevia Therapeutics, Cambridge, MA

E-mail: Dilip.Asthagiri@rice.edu; dheerajstomar@gmail.com

Abstract

The free energies to evacuate the first hydration shell around a solute and a cavity defined by the first hydration shell depend on the system size. This observation interpreted within the quasichemical theory shows that both the hydrophilic and the hydrophobic contributions to hydration depend on the system size, decreasing with increasing system size. Although the net hydration free energy benefits somewhat from the balancing of hydrophilic and hydrophobic contributions, a large system still appears necessary to describe the effect of the solvent on the macromolecule.

Graphical TOC Entry



How many water molecules are needed to simulate a hydrated protein? On the basis of their studies on hemoglobin, Karplus, Meuwly, and coworkers¹ have found that a large system size than conventionally used — about 24 water molecules per protein heavy atom, or about 105,000 water molecules in total — is required to capture the dynamics of deoxy-hemoglobin (PDB: 2DN2). While the statistical resolution of their results have recently been challenged,² the finding by Karplus, Meuwly, and coworkers suggested to us a possible reason why our free energy calculations in conformational switching of protein G_B ³ proved inconclusive. In pursuing this line of research, we have uncovered a hitherto unexpected feature of finite size effect that we discuss below.

In molecular simulations of hydration, using a finite number, N , of solvent molecules is unavoidable. In periodic simulations, there are *implicit* system size effects due to periodicity, for example in pair-correlations⁴ and on electrostatic self-interaction.^{5,6} There are also *explicit* finite size effects that arise from an ensemble dependence,^{7,8} for example, in calculating the compressibility.^{9–11} From the vantage of quasichemical theory theory,^{12–15} we reasoned that such explicit finite size effects should be present in simulations of hydration as well.

To anchor the discussion, first consider the hydration of a simple solute, an imidazole ring (Fig. 1). Once we demarcate the inner-shell domain, the hydration free energy of the solute is

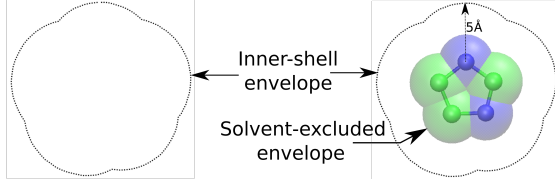


Figure 1: The solute, an imidazole ring, is shown with its associated first hydration or inner shell, defined by the union of overlapping spheres of radius $\lambda = 5 \text{ \AA}$, where λ defines the distance between the heavy atom and water oxygen. (Hydrogens are not shown.) The inner-shell is *open*, exchanging solvent with the bulk. Theory shows that $\lambda \approx 3 \text{ \AA}$ defines the solvent-excluded envelope.

given by quasichemical theory^{12–22} as

$$\mu^{(\text{ex})} = k_B T \ln x_0 - k_B T \ln p_0 + \mu^{(\text{ex})}(n = 0). \quad (1)$$

In Eq. 1, $-k_B T \ln x_0$ is the work done to evacuate the inner shell in the presence of the solute and $-k_B T \ln p_0$ is the corresponding quantity in the absence of the solute; $x_0(p_0)$ is the probability to observe an empty inner shell in the presence (absence) of the solute. $k_B T \ln x_0$ is termed the *chemistry* contribution, since it reflects the contribution to the hydration from short-ranged solute-solvent interactions. It is a measure of the hydrophilic contributions to hydration. $-k_B T \ln p_0$ is the *packing* contribution and is a measure of primitive hydrophobic effects.^{23,24} $\mu^{(\text{ex})}(n = 0) = k_B T \langle e^{\beta \varepsilon} | n = 0 \rangle$ is the contribution to the hydration free energy from solute interaction with the solvent outside the inner-hydration shell; ε is the solute-solvent interaction energy, and the averaging $\langle \dots | n = 0 \rangle$ is performed with solute-solvent thermally coupled, but with the inner-shell empty ($n = 0$) of solvent molecules. As usual $\beta = 1/k_B T$, where T is the temperature and k_B is Boltzmann's constant.

Our earlier studies^{17–22} establish $\lambda = 5 \text{ \AA}$ (Fig. 1) is a conservative definition of the inner shell. For $\lambda \approx 3 \text{ \AA}$ the chemistry contribution is zero, uniquely identifying the domain excluded to the solvent. In our simulations, the inner-outer boundary is defined by a smooth, repulsive potential,²⁵ but this choice is inconse-

quential for the discussion below.

Previously, Hummer et al.⁶ had carefully examined electrostatic contributions in the hydration of imidazole and imidazolium. We follow the same simulation setup (*NVT* ensemble) and same potential model, but obtain the charging free energy using Eq. 1. The free energy of charging the imidazole is given by the difference of $\mu^{(\text{ex})}$ for imidazole and the analog with all charges set to zero ($\mathbf{Q} = \mathbf{0}$). Since the packing contribution cancels in this difference, we need focus only on the chemistry term and the electrostatic contribution to the long-range term. Fig 2 (top panel) shows that the chemistry contribution is system size dependent, but the net electrostatic contribution is not. The excellent agreement with the value computed by Hummer et al.⁶ confirms the internal consistency of our calculation.

Fig 2 (bottom panel) shows that the underlying chemistry (hydrophilic) and packing (hydrophobic) contributions are system size dependent, but these tend to compensate each other in the assessment of the net hydration free energy. However, the compensation is only partial. Thus, for example, for $N = 216$, $\mu^{(\text{ex})} = -10.6 \pm 0.2$, whereas for $N = 512$, $\mu^{(\text{ex})} = -11.7 \pm 0.2$. Note also that for $N = 64$ packing dominates chemistry: this artifact arises due to a constant volume constraint (supplemental information, SI). As our results show, this unphysical behavior is masked in the calculation of $\mu_{\text{elec}}^{(\text{ex})}$.

The linearity of $\ln x_0$ and $\ln p_0$ with v_o/L^3 can be rationalized on the basis of two complementary perspectives. Analysis of fluctuations of number of solvent in a control volume (within a simulation cell) shows that a purely geometric factor of $(1 - v_o/L^3)$ factors from non-ideal contributions.^{10,11} This observation interpreted within a two-moment information theory model^{26,27} then shows that $\ln x_0$ or $\ln p_0$ should have a leading order dependence on v_o/L^3 . Alternatively, assuming ideal gas statistics gives the leading order dependence, we expect $\ln x_0$ (or $\ln p_0$) to depend as $\ln(1 - v_o/L^3) \approx -v_o/L^3$.

We next consider the hydration of the 56-residue protein G_B (PDB: 2LHD), which is one member of a pair of conformational switch pep-

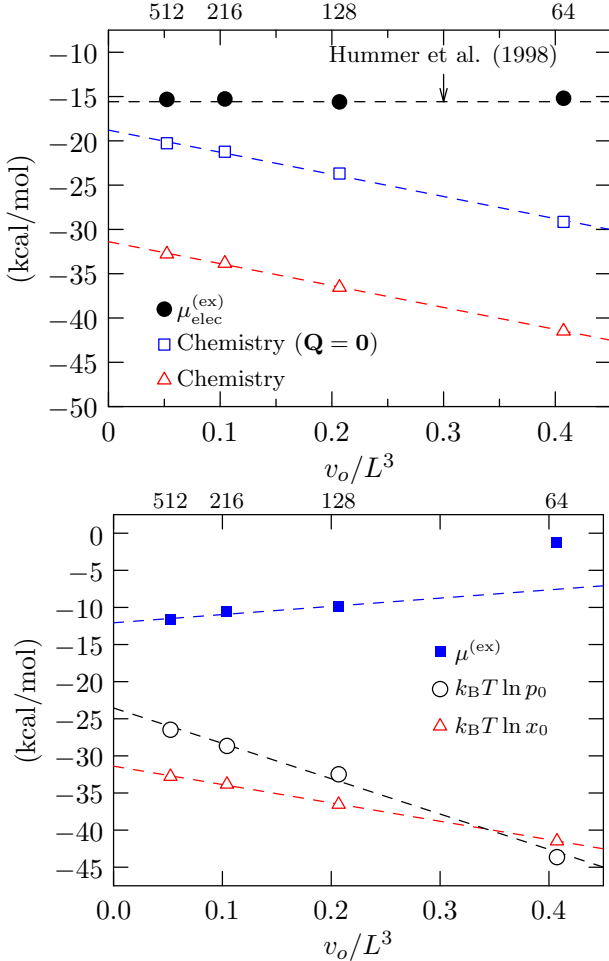


Figure 2: System size dependence of chemistry, packing, and hydration free energy of imidazole. Number of water molecules are noted atop each panel. Statistical uncertainties (1σ) are about the size of the symbols. $v_o = 806.6 \text{ \AA}^3$ is the volume of the inner-shell domain (supplemental information, SI). L^3 is the volume of the cubic simulation system. The long-range contribution (SI) is not shown for clarity. Top: $\mu_{\text{elec}}^{(\text{ex})}$ from Eq. 1. The value reported by Hummer et al. (Fig. 5, Ref. 6) is shown for comparison. Dashed curves are linear fits to the entire data set. Bottom: System size dependence of the net hydration free energy. The extrapolated value is -12.1 kcal/mol . The dashed curves are linear fits excluding $N = 64$.

tides. The protein is also net neutral, helping minimize corrections that are necessary in treating the hydration of a charged molecule.⁶ (G_B is remarkable, for a single mutation flips the conformation of the protein from the $4\beta + \alpha$

fold to a 3α fold.³)

We first establish the reference $\mu_{\text{elec}}^{(\text{ex})}$ (Fig. 3) for G_B on the basis of standard coupling parameter integration (SI). Within statistical uncer-

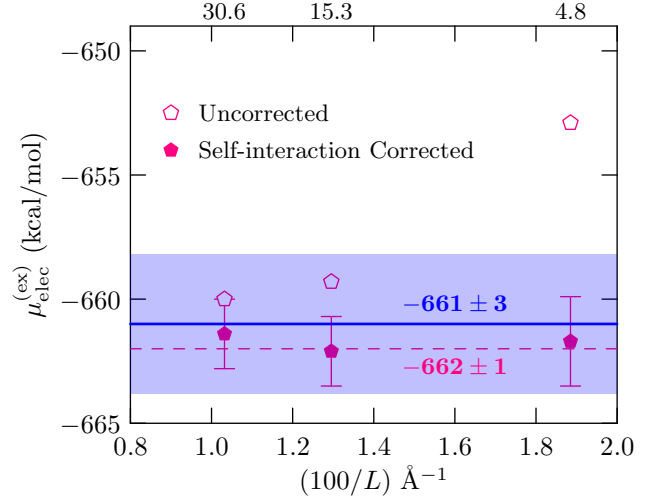


Figure 3: The electrostatic contribution to the free energy of hydration of protein G_B . The open symbols are obtained without applying electrostatic self-interaction corrections, whereas the filled symbols include them (SI). The solid blue line is the result using Eq. 1, with the blue shading indicating the uncertainty. Standard error of the mean is at 2σ . Number of solvent molecules to the nearest thousand is indicated on top. For the largest system, there are about 68 solvent molecules per protein heavy atom.

tainties, $\mu_{\text{elec}}^{(\text{ex})}$ including appropriate corrections (SI) is independent of the system size. We do not include the electrostatic finite size correction because the leading order monopole contribution, zero for G_B , only has a R^2/L^3 dependence,⁶ where R is Born-radius of the solute. The results in Fig. 3 suggest that any finite size correction arising from the dipole contribution should be negligible. Further, just as we found for imidazole, $\mu_{\text{elec}}^{(\text{ex})}$ obtained using the quasichemical approach is in excellent agreement with the result based on coupling parameter integration. Having established this consistency, we next consider the individual packing and chemistry contributions.

Figure 4 (top panel) shows that the (unfavorable) packing or primitive hydrophobic contri-

bution becomes *weaker* with increasing system size as does the (favorable) chemistry contribution (Fig. 4, bottom panel). These trends are similar to that for imidazole.

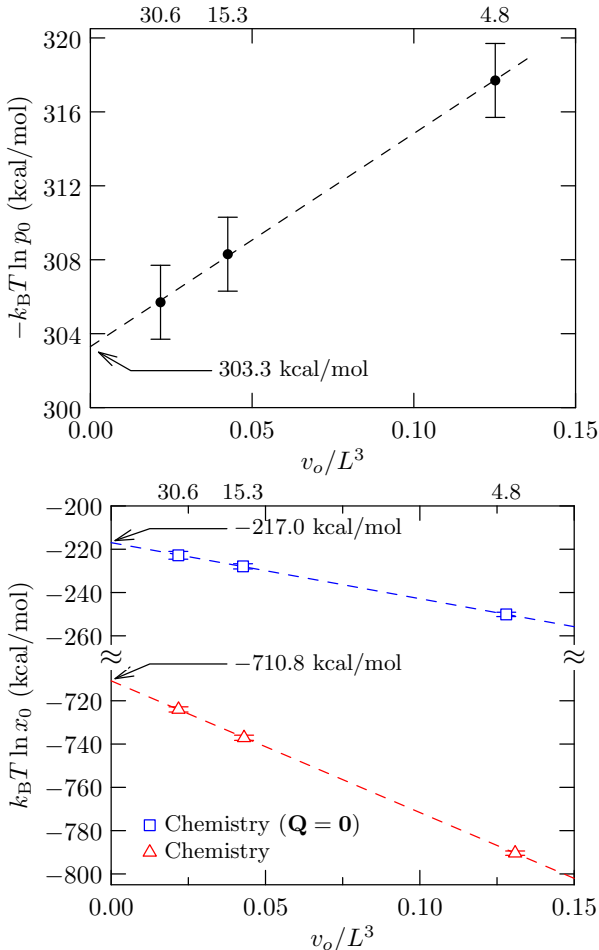


Figure 4: Top: The packing (primitive hydrophobic) contribution to $\mu^{(\text{ex})}$. Bottom: The chemistry contribution to $\mu^{(\text{ex})}$ for G_B and its $\mathbf{Q} = \mathbf{0}$ analog. $v_o = 20040.4 \text{ \AA}^3$. Standard error of the mean is shown at 2σ .

Figure 5 gives the hydration free energy of the G_B and its $\mathbf{Q} = \mathbf{0}$ analog. The hydration free energy includes the long-range contribution, $\mu^{(\text{ex})}(n = 0)$, which are only weakly dependent on the system size (SI). From the extrapolated $L \rightarrow \infty$ value, we estimate the charging free energy $-628 - 33 = -661 \pm 3 (2\sigma)$ kcal/mol noted in Fig. 3.

The results above definitively establish that the first hydration shell occupancy, and hence the hydration thermodynamics itself, is sensitive to the size of the simulation system. The

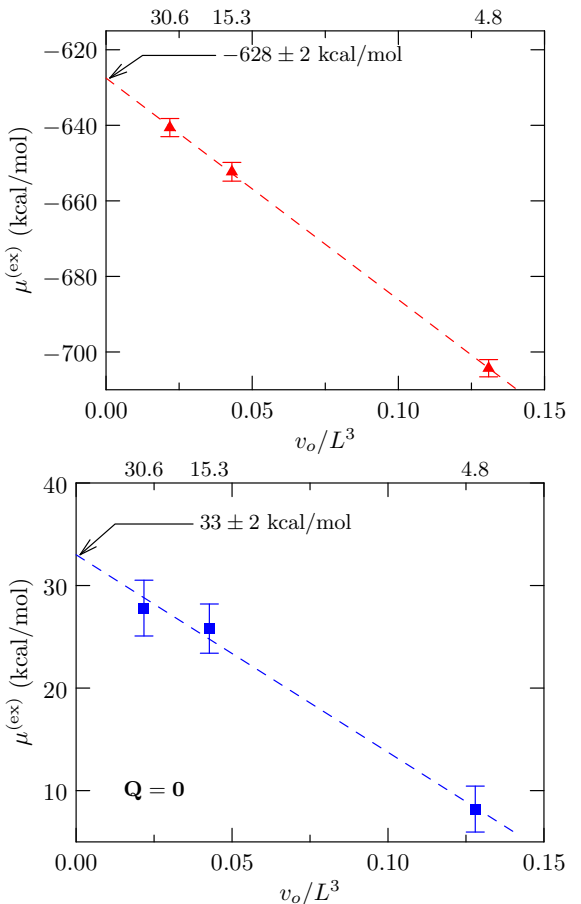


Figure 5: Hydration free energy of G_B (top) and its $\mathbf{Q} = \mathbf{0}$ analog (bottom). Electrostatic self-interaction corrections are included in the free energy calculation of G_B . Standard error of the mean is shown at 2σ .

system size dependence noted here is quite general and arises because the first shell is an open system that exchanges solvent with the bath. This feature, one that is made explicit by quasi-chemical theory,^{12–15} has implications for *all simulation studies of hydration*.

The present work suggests that the observations by Karplus, Meuwly, and coworkers¹ merits further study, but their rationalization of enhanced hydrophobic hydration in larger systems should be reconsidered. We find that the hydrophobic contribution is *weakened* with increasing system size, consistent with the intuition of enhanced solvent density fluctuations at the scale of the observation volume in a larger system. However, the hydrophilic (chemistry) contribution becomes less favorable as

well. That is the solvent is less effective in prying apart or loosening the protein structure, and this effect dominates the weakening of hydrophobic hydration, as our recent studies emphasize.^{19–22} This combined effect should stabilize the conformation (assuming no change in intra-molecular interactions).

The criticisms of Ref. 1 by Gapsys and de Groot, especially their analysis based on model compounds such as alanine dipeptide, also merit serious consideration. We suspect that in conformational transitions the finite size effects noted here are muted. Exploring such issues in biomolecular folding and assembly is left for future studies.

Our observations are also likely important in *ab initio* simulation studies, since these still rely on rather small systems. We hope our work proves useful to researchers in this area.

Acknowledgement We gratefully acknowledge computing support from National Energy Research Scientific Computing Center, which is supported by the Office of Science of the U.S. Department of Energy under Contract # DE-AC02-05CH11231. D. A. thanks Lawrence Pratt and Walter Chapman for helpful comments and encouragement.

Supporting Information Available

The following files are available free of charge. Information on the simulation systems, quasi-chemical calculations, calculation of reference value of charging free energy, tabulated data, and analog of Fig. 2 for G_B .

References

- (1) El Hage, K.; Hédin, F.; Gupta, P. K.; Meuwly, M.; Karplus, M. Valid Molecular Dynamics Simulations of Human Hemoglobin Require a Surprisingly Large Box Size. *eLife* **2018**, *e35560*.
- (2) Gapsys, V.; de Groot, B. L. Comment on ‘Valid Molecular Dynamics Simulations of Human Hemoglobin Require a Surprisingly Large Box Size’. *bioRxiv*. DOI: [10.1101/563064](https://doi.org/10.1101/563064) **2019**,
- (3) Alexander, P. A.; He, Y.; Chen, Y.; Orban, J.; Bryan, P. N. A Minimal Sequence Code for Switching Protein Structure and Function. *Proc. Natl. Acad. Sci. USA* **2009**, *106*, 21149–21154.
- (4) Pratt, L. R.; Haan, S. W. Effects of Periodic Boundary Conditions on Equilibrium Properties of Computer Simulated Fluids. I. Theory. *J. Chem. Phys.* **1981**, *74*, 1864–1872.
- (5) Hummer, G.; Pratt, L. R.; Garcia, A. E. Free Energy of Ionic Hydration. *J. Phys. Chem.* **1996**, *1206*–1215.
- (6) Hummer, G.; Pratt, L. R.; Garcia, A. E. Molecular Theories and Simulation of Ions and Polar Molecules in Water. *J. Phys. Chem. A* **1998**, *102*, 7885–7895.
- (7) Lebowitz, J. L.; Percus, J. K. Thermodynamic Properties of Small Systems. *Phys. Rev.* **1961**, *124*, 1673–1681.
- (8) Lebowitz, J. L.; Percus, J. K.; Verlet, L. Ensemble Dependence of Fluctuations with Application to Machine Computation. *Phys. Rev.* **1967**, *153*, 250–154.
- (9) Salacuse, J. J.; Denton, A. R.; Egelstaff, P. A. Finite-size Effects in Molecular Dynamics Simulations: Static Structure Factor and Compressibility. I. Theoretical Method. *Phys. Rev. E* **1996**, *53*, 2382–2389.
- (10) Román, F. L.; González, A.; White, J. A.; Velasco, S. Fluctuations in the Number of Particles of the Ideal Gas: A Simple Example of Explicit Finite-size Effects. *Am. J. Phys.* **1999**, *67*, 1149–1151.
- (11) Villamaina, D.; Trizac, E. Thinking Outside The Box: Fluctuations and Finite Size Effects. *Eur. J. Phys.* **2014**, *35*, 035011.

- (12) Pratt, L. R.; Rempe, S. B. In *Simulation and theory of electrostatic interactions in solution. Computational chemistry, biophysics, and aqueous solutions*; Pratt, L. R., Hummer, G., Eds.; AIP Conference Proceedings; American Institute of Physics: Melville, NY, 1999; Vol. 492; pp 172–201, dx.doi.org/10.1063/1.1301528.
- (13) Paulaitis, M. E.; Pratt, L. R. Hydration Theory for Molecular Biophysics. *Adv. Prot. Chem.* **2002**, *62*, 283–310.
- (14) Beck, T. L.; Paulaitis, M. E.; Pratt, L. R. *The Potential Distribution Theorem and Models of Molecular Solutions*; Cambridge University Press: Cambridge, UK, 2006.
- (15) Pratt, L. R.; Asthagiri, D. In *Free energy calculations: Theory and applications in chemistry and biology*; Chipot, C., Pohorille, A., Eds.; Springer series in Chemical Physics; Springer: Berlin, DE, 2007; Vol. 86; Chapter 9, pp 323–351.
- (16) Weber, V.; Asthagiri, D. Regularizing Binding Energy Distributions and the Hydration Free Energy of Protein Cytochrome C from All-Atom Simulations. *J. Chem. Theory Comput.* **2012**, *8*, 3409–3415.
- (17) Tomar, D. S.; Weber, V.; Asthagiri, D. Solvation Free Energy of the Peptide Group: Its Model Dependence and Implications for the Additive Transfer Free Energy Model. *Biophys. J.* **2013**, *105*, 1482–1490.
- (18) Tomar, D. S.; Weber, V.; Pettitt, B. M.; Asthagiri, D. Conditional Solvation Thermodynamics of Isoleucine in Model Peptides and the Limitations of the Group-Transfer Model. *J. Phys. Chem. B* **2014**, *118*, 4080–4087.
- (19) Tomar, D. S.; Weber, W.; Pettitt, M. B.; Asthagiri, D. Importance of Hydrophilic Hydration and Intramolecular Interactions in the Thermodynamics of Helix-Coil Transition and Helix-Helix Assembly in a Deca-Alanine Peptide. *J. Phys. Chem. B* **2016**, *120*, 69–76.
- (20) Asthagiri, D.; Karandur, D.; Tomar, D. S.; Pettitt, B. M. Intramolecular Interactions Overcome Hydration to Drive the Collapse Transition of Gly₁₅. *J. Phys. Chem. B* **2017**, *121*, 8078–8084.
- (21) Tomar, D. S.; Ramesh, N.; Asthagiri, D. Solvophobic and Solvophilic Contributions in the Water-To-Aqueous Guanidinium Chloride Transfer Free Energy of Model Peptides. *J. Chem. Phys.* **2018**, *148*, 222822.
- (22) Tomar, D. S.; Paulaitis, M. E.; Pratt, L. R.; Asthagiri, D. Long-Range Interactions Dominate the Inverse-temperature Dependence of Polypeptide Hydration Free Energies. *arXiv:1812.06913v3* **2019**,
- (23) Pratt, L. R.; Pohorille, A. Theory of Hydrophobicity: Transient Cavities in Molecular Liquids. *Proc. Natl. Acad. Sci. USA* **1992**, *89*, 2995–2999.
- (24) Pratt, L. R. Molecular Theory of Hydrophobic Effects: “She Is Too Mean To Have Her Name Repeated”. *Ann. Rev. Phys. Chem.* **2002**, *53*, 409–436.
- (25) Chempath, S.; Pratt, L. R.; Paulaitis, M. E. Quasi-chemical Theory with a Soft Cutoff. *J. Chem. Phys.* **2009**, *130*, 054113.
- (26) Hummer, G.; Garde, S.; Garcia, A. E.; Pohorille, A.; Pratt, L. R. An Information Theory Model of Hydrophobic Interactions. *Proc. Natl. Acad. Sci. USA* **1996**, *93*, 8951–8955.
- (27) Hummer, G.; Garde, S.; Garcia, A. E.; Paulaitis, M. E.; Pratt, L. R. Hydrophobic Effects on a Molecular Scale. *J. Phys. Chem. B* **1998**, *102*, 10469–10482.

Supporting information for: System size dependence of hydration shell occupancy

D. Asthagiri^{*,†} and Dheeraj Singh Tomar^{*,‡}

[†]*Department of Chemical and Biomolecular Engineering, Rice University, Houston, TX*

[‡]*Akrevia Therapeutics, Cambridge, MA*

E-mail: Dilip.Asthagiri@rice.edu; dheerajstomar@gmail.com

System

All the simulations are performed using the NAMD code.¹ Since solute conformation was frozen and a rigid water model is used, we use a 2 fs time step for integrating the equations of motion.

Imidazole

The parameters for imidazole were obtained from Ref. 2; consistent with that work, water was modeled using the SPC/E potential.³ Following Ref. 2, both neat water and water with one imidazole was modeled under NVT conditions. Neat water was simulated at a density of 0.997 gm/cc and the partial molar volume of imidazole was chosen as 2 times that of bulk water. The temperature of 298 K was enforced using a Langevin thermostat. The solvent box contained $N = 64, 128, 256$, or 512 molecules.

For $N = 64$, the Lennard-Jones interactions were switched to zero between 4.215 Å and 5.215 Å. For the other systems, the Lennard-Jones interactions were switched to zero between 6.63 Å and 7.03 Å. Electrostatic interactions were treated using particle mesh Ewald with a grid spacing of 0.5 Å.

Protein G_B

The protein (PDB: 2LHD) was modeled using version 36m of the CHARMM forcefield⁴⁻⁷ and water was modeled using CHARMM-modified TIP3P potential.^{8,9} Charged residues were modeled in their standard ionization state at pH 7. The terminal residues were modeled in their ionized states. The protein is net neutral under the simulated conditions.

First all the NMR structures in the PDB file were energy minimized: 500 steps fixing protein heavy atoms and a subsequent 500 steps without any constraints. We then calculate their combined intra-molecular plus solvation free energy (obtained using the GB/SA model^{10,11}), i.e. the free energy in solution. On this basis, we chose model 3, as it had the lowest free energy.

The solvent box comprises $N = 4775, 15302$, or 30616 waters. For all the systems, the Lennard-Jones interactions were switched to zero between 12 \AA and 13 \AA and electrostatic interactions were treated using particle mesh Ewald with a grid spacing of 0.5 \AA . All systems were modeled under NpT conditions, with the temperature of 298 K controlled using a Langevin thermostat and the pressure of 1 atm . controlled using a Langevin barostat.¹²

Quasichemical theory

The calculation of the hydration free energy components above closely follows earlier studies.^{13–19} Here we present only the points needed to follow the main article. Once we demarcate the inner-shell region of size λ , $\mu^{(ex)}$ is given by

$$\mu^{(ex)} = k_B T \ln x_0(\lambda) - k_B T \ln p_0(\lambda) + \mu^{(ex)}(n = 0|\lambda). \quad (\text{S.1})$$

We apply atom-centered fields, $\phi(r; \lambda)$, to carve a molecular cavity in the liquid or around the solute;^{14–19} r is the distance to the oxygen atom of water and λ is a parameter that defines the range of the field. We find that $\lambda \approx 5 \text{ \AA}$ ensures that the conditional (i.e. $n = 0|\lambda$) binding energy distribution is gaussian to a good approximation. We denote this range as λ_G . The largest value of λ , labelled λ_{SE} , for which the chemistry contribution is zero has a special meaning. It demarcates the domain which is excluded to the solvent. *For the given forcefield and solute geometry, this surface is uniquely defined.*¹⁶ We find that $\lambda_{\text{SE}} \approx 3 \text{ \AA}$. With this choice, Eq. S.1 can be rearranged as,

$$\mu^{(ex)} = \underbrace{k_B T \ln \left[x_0(\lambda_G) \frac{p_0(\lambda_{\text{SE}})}{p_0(\lambda_G)} \right]}_{\text{revised chemistry}} - \underbrace{k_B T \ln p_0(\lambda_{\text{SE}})}_{\text{SE packing}} + \underbrace{\mu^{(ex)}(n = 0|\lambda_G)}_{\text{long-range}}. \quad (\text{S.2})$$

The term identified as revised chemistry has the following physical meaning. It is the free energy gained in allowing the solvent into the inner shell relative to the value for a solute

that simply excludes the solvent. This term explicates the role of short-range solute-solvent attractive interactions on hydration. Interestingly, the range between $\lambda_{SE} = 3 \text{ \AA}$ and $\lambda_G = 5 \text{ \AA}$ corresponds to the first hydration shell for a methane carbon²⁰ and is an approximate descriptor of the first hydration shell of groups containing nitrogen and oxygen heavy atoms.

For simplicity, in the main text we present results exclusively based on λ_G . For the protein, the dependence of chemistry and revised chemistry on system size is the same, as should be expected based on their physical meaning. However for imidazole, this is not be the case, since the calculations are under *NVT* conditions. Specifically, moving the solvent interface away from the solute costs substantially more²¹ under *NVT* conditions than under *NpT* conditions, skewing the relative balance of chemistry and packing. This is the reason why for $N = 64$, packing dominates chemistry (Fig. 2, main text), a behavior that is unphysical for a polar compound. For the same reason, for imidazole simulated under *NVT* conditions, chemistry and revised chemistry contributions have different dependencies on system size.

Chemistry and packing contributions

To build the field to its eventual range of $\lambda_G = 5 \text{ \AA}$, we progressively apply the field and for every unit \AA increment in the range, we compute the work using a seven-point Gauss-Legendre quadrature.²² Error analysis and error propagation was performed as before:¹³⁻¹⁹ the standard error of the mean force was obtained using the Friedberg-Cameron algorithm^{23,24} and in adding multiple quantities, the errors were propagated using variance-addition rules.

The starting configuration for each λ point is obtained from the ending configuration of the previous point in the chain of states. For the packing contributions, a total of 35 Gauss points span $\lambda \in [0, 5]$. For the chemistry contribution, since solvent never enters $\lambda < 2.5 \text{ \AA}$, we simulate $\lambda \in [2, 5]$ for a total of 21 Gauss points.

Imidazole

We perform 1 ns of simulation at each λ and use the data from the last 0.5 ns for analysis. Force data is archived every 50 fs for analysis.

G_B

We perform 0.8 ns of simulation at each λ and use the data from the last 0.4 ns for analysis. Force data is archived every 50 fs for analysis.

The packing calculation for G_B includes additional subtleties. To prevent water molecules from being trapped inside the inner-shell envelope, we do the packing calculation in three stages, corresponding to the β_1 , α , and β_2 secondary structural domains of the protein (Fig. S1). We first create the λ_{SE} cavity for β_1 . Next, with the β_1 cavity in place, we

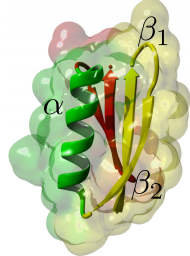


Figure S1: The structure of protein G_B showing the main secondary structural elements.

create the λ_{SE} cavity for α . Finally, we create the β_2 cavity in the presence of the λ_{SE} cavities for β_1 and α . With the λ_{SE} cavity for the entire protein in place, we create the λ_G cavity. Such an approach also provides information on the energetics of conditional cavity formation to accommodate each secondary structural element and proves helpful in monitoring convergence of the calculations.

Long-range contribution

Throughout, solute-solvent binding energies were obtained using the PAIRINTERACTION module in NAMD.

The conditional solute-solvent binding energy distribution is $P(\varepsilon|n = 0)$, where ε is the solute-solvent binding energy. For $P(\varepsilon|n = 0)$ described by a Gaussian, we have^{25,26}

$$\mu^{\text{ex}}(n = 0) = \langle \varepsilon|n = 0 \rangle + \frac{\beta}{2}\sigma^2 \quad (\text{S.3})$$

In the above equations, $\langle \varepsilon|n = 0 \rangle$ is the mean binding energy and σ^2 is the variance of the distribution, with solvent prohibited from entering the inner shell. For characterizing $P(\varepsilon|n = 0)$, the starting configuration for the $\lambda_G = 5$ Å simulation was obtained from the endpoint of the Gauss-Legendre procedure for the chemistry calculation.

Imidazole

The system with λ_G was simulated for 2 ns and frames were saved every 200 fs. We used the last 9500 frames for analysis. The long-range contribution includes both electrostatics and van der Waals interactions. The individual distributions are also Gaussian, serving as a further consistency check of the simulations (see, for example, Ref. 14).

\mathbf{G}_B

Since the protein has a very large dipole moment (≈ 150 D), we use the Gaussian model only for van der Waals interactions. The $\mathbf{Q} = \mathbf{0}$ system with λ_G was simulated for 2 ns and frames saved every 200 fs. We used the last 9000 frames for calculating the van der Waals contribution using the Gaussian model. For the electrostatic contributions, we use a 3-point quadrature rule.²² At each Gauss point, the system was simulated for 0.7 ns and frames saved every 200 fs for further analysis. In contrast to our earlier studies on simpler peptides,^{16–19} we find that the linear response result (the Gaussian model result) differs from the 3-point result by between 3 and 4 kcal/mol, outside the uncertainty of 0.2 kcal/mol for the quadrature-based result (see tables below).

Reference free energy of charging

For charging a solute from $\mathbf{Q} = \mathbf{0}$ to the final charge distribution \mathbf{Q} , we use well-documented ideas.^{2,22} Let $\phi(\mathbf{r}_{\alpha\beta})$ be the Ewald potential between partial charges q_α and q_β at locations \mathbf{r}_α and \mathbf{r}_β in the solute. (Please note that the solute is treated as a rigid entity in our simulations.) Then the free energy of charging the solute is given by²

$$\mu^{(\text{ex})} = \mu_{\text{sim}}^{(\text{ex})} + \frac{1}{2} \sum_{\substack{\alpha, \beta \\ \alpha \neq \beta}} q_\alpha q_\beta \left[\phi(\mathbf{r}) - \frac{1}{|\mathbf{r}_{\alpha\beta}|} \right] + \frac{1}{2} \sum_\alpha q_\alpha^2 \xi \quad (\text{S.4})$$

where $\xi = -2.827297/L$ is the Wigner potential for a cubic cell of length L . The second and third terms together constitute the self-interaction correction noted in the main text. The second term accounts for the interaction between partial charge sites on the solute and its periodic images. The third term is the ionic self-interaction contribution. $\mu_{\text{sim}}^{(\text{ex})}$ is the contribution to the hydration free energy from solute interaction with the solvent, and it is this term that is obtained using quadratures. For constant pressure simulations, the self-interaction contribution should be averaged as the simulation volume fluctuates. In practice, for the box sizes considered in this work, we find that using a box size based on the average volume suffices in computing the correction. (While strictly not correct, this procedure has the virtue of simplicity and the error due to this simplification is insignificant.) The self-interaction contributions were obtained using an in-house Ewald summation code; the Ewald screening parameter and number of k-space vectors follow the recommendation in Ref. 2.

For imidazole, we took the reference free energy value from Ref. 2. For G_B , at each Gauss point we simulated the system for 0.6 ns, saving data every 200 fs. We used the last 2500 frames for analysis.

Molecular volumes

To compute the volume associated with an envelope defined by λ , we assign the radius λ to the solute heavy atoms. We then use the MSMS code²⁷ to calculate the *solvent excluded* volume for that envelope.

Data

Throughout, energy values are reported in kcal/mol.

Imidazole

Table S.I: Packing contribution for $\lambda_G = 5 \text{ \AA}$ and $\lambda_{SE} = 3 \text{ \AA}$. Standard error of the mean is at 1σ .

N	$L (\text{\AA})$	Packing	
		λ_G	λ_{SE}
512	24.859	26.5 ± 0.1	6.03 ± 0.05
256	19.730	28.7 ± 0.2	6.09 ± 0.05
128	15.660	32.5 ± 0.1	6.14 ± 0.07
64	12.429	43.6 ± 0.2	6.45 ± 0.05

Table S.II: Chemistry and long-range contributions for the \mathbf{Q} and $\mathbf{Q} = 0$ cases. Elec_{corr} is the Ewald self-interaction correction. Standard error of the mean is at 1σ .

N	$L (\text{\AA})$	Chemistry			Long-range		
		\mathbf{Q}	$\mathbf{Q} = 0$	Elec_{corr}	\mathbf{Q}	$\mathbf{Q} = 0$	
512	24.891	-32.8 ± 0.1	-20.3 ± 0.1	-0.06	-5.27 ± 0.06	-2.56	
256	19.782	-33.8 ± 0.1	-21.2 ± 0.1	-0.12	-5.25 ± 0.06	-2.73	
128	15.741	-36.5 ± 0.1	-23.7 ± 0.1	-0.24	-5.55 ± 0.05	-3.07	
64	12.557	-41.5 ± 0.1	-29.2 ± 0.1	-0.48	-2.92 ± 0.05	-0.55	

G_B

Table S.III: Free energy of charging G_B from $Q = 0$ to the final partial charge distribution Q using a 3-point Gauss-Legendre quadrature. $\mu_{\text{sim}}^{(\text{ex})}$ is the solute-solvent interaction contribution to the free energy. $\text{Elec}_{\text{corr}}$ is the self-interaction correction (Eq. S.4). The given box length is the box length based on the average volume for the system at the final charge distribution. The correction is evaluated using this value of the box length. Standard error of the mean is at 1σ .

N	L (Å)	$\mu_{\text{sim}}^{(\text{ex})}$	$\text{Elec}_{\text{corr}}$	$\mu_{\text{elec}}^{(\text{ex})}$
30616	96.9	-660.0 ± 0.7	-1.4	-661.4 ± 0.7
15302	77.2	-659.3 ± 0.7	-2.8	-662.1 ± 0.7
4775	53.1	-652.9 ± 0.9	-8.8	-661.7 ± 0.9

Table S.IV: Packing contribution for $\lambda_G = 5$ Å and $\lambda_{SE} = 3$ Å. Standard error of the mean is at 1σ .

N	L (Å)	Packing	
		λ_G	λ_{SE}
30616	97.41	305.7 ± 1.0	218.5 ± 1.0
15302	77.85	308.3 ± 1.0	219.3 ± 1.0
4775	54.3	317.7 ± 1.0	222.2 ± 1.0

Table S.V: Chemistry and long-range electrostatic (Elec.) and van der Waals (vdW) contributions in the net hydration free energy, $\mu^{(ex)}$, of G_B . The long-range electrostatic contribution is obtained using a 3-point Gauss-Legendre quadrature. The linear response (or gaussian) value for the electrostatic contribution is noted in parenthesis. Standard error of the mean is at 1σ .

N	L (Å)	Chemistry	Long-range				$\mu^{(ex)}$
			Elec.	vdW	$Elec_{corr}$		
30616	97.2	-724.0 ± 0.6	-165.8 ± 0.2 (-161.8)	-55.1 ± 0.2	-1.4	-640.6	
15302	77.5	-737.1 ± 0.6	-166.1 ± 0.3 (-162.3)	-54.6 ± 0.3	-2.8	-652.3	
4775	53.5	-790.4 ± 0.5	-163.4 ± 0.2 (-160.3)	-59.4 ± 0.1	-8.8	-704.3	

Tables S.IV and S.V can be used to calculate the revised chemistry contribution. For example, for $N = 4775$, the revised chemistry contribution is $-790.4 + 317.7 - 222.2 = -694.9$ kcal/mol. This is the work done in allowing water molecules to enter the inner-shell of G_B relative to the case when the repulsive hard-core solute. For G_B , the revised chemistry contribution has the same qualitative dependence on v_o/L^3 as the chemistry contribution (Fig. 4, main text).

Table S.VI: Chemistry and long-range (vdW) contributions in the net hydration free energy, $\mu^{(ex)}$, of the $Q = 0$ analog of G_B . Standard error of the mean is at 1σ .

N	L (Å)	Chemistry	vdW	$\mu^{(ex)}$
30616	97.3	-222.8 ± 0.9	-55.1 ± 0.2	27.8
15302	77.7	-227.9 ± 0.6	-54.6 ± 0.3	25.8
4775	53.9	-250.1 ± 0.5	-59.4 ± 0.1	8.2

Free energy of charging G_B

In the main text, we obtain the free energy of charging G_B from the difference of the (absolute) hydration free energies of G_B and its $\mathbf{Q} = \mathbf{0}$ analog. The absolute hydration free energies were obtained from the $L \rightarrow \infty$ extrapolation, and using those values we had the result $\mu_{\text{elec}}^{(\text{ex})} = -628 - 33 = -661 \pm 3 (2\sigma)$ kcal/mol.

As we did for imidazole, we can also find the charging free energy from the difference of the chemistry contributions plus the long-range electrostatic and self-interaction correction values (Table S.V). This calculation also proves illuminating. As Fig. S2 shows, the $L \rightarrow \infty$ value is in excellent agreement with the average value obtained from coupling parameter integration procedure (Table S.III).

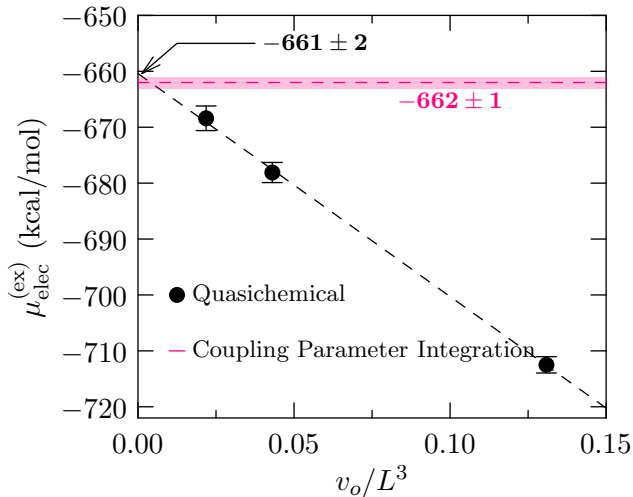


Figure S2: System size dependence of the charging free energy for G_B . The quasichemical value includes self-interaction corrections.

But there is an important contrast to me made with imidazole. Unlike the case for imidazole (Fig. 2), even after including self-interaction corrections, we find that the charging free energy (from the quasichemical procedure) has a strong system size dependence. There are two reasons for this: (1) the calculations are under NpT conditions and (2) in the charging of the solute with the empty inner-shell, we will likely need to consider electrostatic *finite size* corrections, since the solute with an empty $\lambda = 5$ Å envelope will occupy a much

larger volume in the simulation cell. (The volume of the λ_G envelope is nearly 1.8 times that of the λ_{SE} envelope.) For an ion of Born radius R , Hummer et al. (Ref. 2) showed that the *finite size* correction will scale as R^2/L^3 . Analytically working out the scaling for a protein with its partial charge distribution is an daunting task, but it may be possible to estimate the correction numerically (by solving Poisson's equation). While we have not attempted this, by analogy with the ion case we expect the correction to be a positive contribution that is inversely proportional to the box volume, i.e. the quasichemical value should be below the coupling parameter value. The trend in Fig. S2 is consistent with this expectation. Further exploration of the finite size correction is left for future studies.

References

- (1) Kale, L.; Skeel, R.; Bhandarkar, M.; Brunner, R.; Gursoy, A.; Krawetz, N.; Phillips, J.; Shinozaki, A.; Varadarajan, K.; Schulten, K. NAMD2: Greater scalability for parallel molecular dynamics. *J. Comput. Phys.* **1999**, *151*, 283.
- (2) Hummer, G.; Pratt, L. R.; Garcia, A. E. Molecular Theories and Simulation of Ions and Polar Molecules in Water. *J. Phys. Chem. A* **1998**, *102*, 7885–7895.
- (3) Berendsen, H. J. C.; Grigera, J. R.; Straatsma, T. P. The missing term in effective pair potentials. *J. Phys. Chem.* **1987**, *91*, 6269–6271.
- (4) MacKerell, Jr., A. D.; Bashford, D.; Bellott, M.; Dunbrack, Jr., R. L.; Evanseck, J. D.; Field, M. J.; Fischer, S.; Gao, J.; Guo, H.; Ha, S. et al. All-Atom Empirical Potential for Molecular Modeling and Dynamics Studies of Proteins. *J. Phys. Chem. B* **1998**, *102*, 3586–3616.
- (5) MacKerell, Jr., A. D.; Feig, M.; Brooks, III, C. L. Improved treatment of the protein backbone in empirical force fields. *J. Am. Chem. Soc.* **2004**, *126*, 698–699.
- (6) Best, R. B.; Zhu, X.; Shim, J.; Lopes, P.; Mittal, J.; Feig, M.; MacKerell, Jr., A. D. Optimization of the additive CHARMM all-atom protein force field targeting improved sampling of the backbone phi, psi and sidechain χ_1 and χ_2 dihedral angles. *J. Chem. Theory Comput.* **2013**, *8*, 3257–3273.
- (7) Huang, J.; Rauscher, S.; Nawrocki, G.; Ran, T.; Feig, M.; de Groot, B. L.; Grubmüller, H.; MacKerell, Jr., A. D. CHARMM36m: an improved force field for folded and intrinsically disordered proteins. *Nature Methods* **2017**, *14*, 71–73.
- (8) Jorgensen, W.; Chandrasekhar, J.; Madura, J. D.; Impey, R. W.; Klein, M. L. Comparison of Simple Potential Functions for Simulating Liquid Water. *J. Chem. Phys.* **1983**, *79*, 926–935.

- (9) Neria, E.; Fischer, S.; Karplus, M. Simulation of Activation Free Energies in Molecular Systems. *J. Chem. Phys.* **1996**, *105*, 1902–1921.
- (10) Still, W. C.; Tempczyk, A.; Hawley, R. C.; Hendrickson, T. Semianalytical treatment of solvation for molecular mechanics and dynamics. *J. Am. Chem. Soc.* **1990**, *112*, 6127–6129.
- (11) Onufriev, A.; Bashford, D.; Case, D. A. Modification of the generalized Born model suitable for macromolecules. *J. Phys. Chem. B* **2000**, *104*, 3712–3720.
- (12) Feller, S. E.; Zhang, Y.; Pastor, R. W.; Brooks, B. R. Constant pressure molecular dynamics simulation: The Langevin piston method. *J. Chem. Phys.* **1995**, *103*, 4613–4621.
- (13) Weber, V.; Asthagiri, D. Regularizing Binding Energy Distributions and the Hydration Free Energy of Protein Cytochrome C from All-Atom Simulations. *J. Chem. Theory Comput.* **2012**, *8*, 3409–3415.
- (14) Tomar, D. S.; Weber, V.; Asthagiri, D. Solvation Free Energy of the Peptide Group: Its Model Dependence and Implications for the Additive Transfer Free Energy Model. *Biophys. J.* **2013**, *105*, 1482–1490.
- (15) Tomar, D. S.; Weber, V.; Pettitt, B. M.; Asthagiri, D. Conditional Solvation Thermodynamics of Isoleucine in Model Peptides and the Limitations of the Group-Transfer Model. *J. Phys. Chem. B* **2014**, *118*, 4080–4087.
- (16) Tomar, D. S.; Weber, W.; Pettitt, M. B.; Asthagiri, D. Importance of Hydrophilic Hydration and Intramolecular Interactions in the Thermodynamics of Helix-Coil Transition and Helix-Helix Assembly in a Deca-Alanine Peptide. *J. Phys. Chem. B* **2016**, *120*, 69–76.

- (17) Asthagiri, D.; Karandur, D.; Tomar, D. S.; Pettitt, B. M. Intramolecular Interactions Overcome Hydration to Drive the Collapse Transition of Gly₁₅. *J. Phys. Chem. B* **2017**, *121*, 8078–8084.
- (18) Tomar, D. S.; Ramesh, N.; Asthagiri, D. Solvophobic and Solvophilic Contributions in the Water-To-Aqueous Guanidinium Chloride Transfer Free Energy of Model Peptides. *J. Chem. Phys.* **2018**, *148*, 222822.
- (19) Tomar, D. S.; Paulaitis, M. E.; Pratt, L. R.; Asthagiri, D. Long-Range Interactions Dominate the Inverse-temperature Dependence of Polypeptide Hydration Free Energies. *arXiv:1812.06913v3* **2019**,
- (20) Asthagiri, D.; Merchant, S.; Pratt, L. R. Role of Attractive Methane-Water Interactions in the Potential of Mean Force Between Methane Molecules in Water. *J. Chem. Phys.* **2008**, *128*, 244512.
- (21) Merchant, S.; Shah, J. K.; Asthagiri, D. Water coordination structures and the excess free energy of the liquid. *J. Chem. Phys.* **2010**, *134*, 124514.
- (22) Hummer, G.; Szabo, A. Calculation of free-energy differences from computer simulations of initial and final states. *J. Chem. Phys.* **1996**, *105*, 2004–2010.
- (23) Friedberg, R.; Cameron, J. E. Test of the Monte Carlo method: fast simulation of a small Ising lattic. *J. Chem. Phys.* **1970**, *52*, 6049–6058.
- (24) Allen, M. P.; Tildesley, D. J. *Computer simulation of liquids*; Oxford University Press, 1987; Chapter 6. How to analyze the results, pp 192–195.
- (25) Beck, T. L.; Paulaitis, M. E.; Pratt, L. R. *The Potential Distribution Theorem and Models of Molecular Solutions*; Cambridge University Press: Cambridge, UK, 2006.
- (26) Pratt, L. R.; Asthagiri, D. In *Free energy calculations: Theory and applications in*

chemistry and biology; Chipot, C., Pohorille, A., Eds.; Springer series in Chemical Physics; Springer: Berlin, DE, 2007; Vol. 86; Chapter 9, pp 323–351.

- (27) Sanner, M.; Olson, A. J.; Spehner, J. C. Reduced Surface: An Efficient Way to Compute Molecular Surfaces. *Biopolymers* **1996**, *38*, 305–320.